Since January 2020 Elsevier has created a COVID-19 resource centre with free information in English and Mandarin on the novel coronavirus COVID-19. The COVID-19 resource centre is hosted on Elsevier Connect, the company's public news and information website.

Journal of Cleaner Production 375 (2022) 134086

Contents lists available at ScienceDirect

Journal of Cleaner Production

journal homepage: www.elsevier.com/locate/jclepro

Reusing COVID-19 disposable nitrile gloves to improve the mechanical properties of expansive clay subgrade: An innovative medical waste solution

Jiasheng Zhu [a], Mohammad Saberian [a,1], Salpadoru Tholkamudalige Anupiya.M. Perera [a], Rajeev Roychand [a], Jie Li [a,*], George Wang [b]

[a] School of Engineering, RMIT University, Melbourne, Victoria, Australia
[b] College of Engineering and Technology, East Carolina University, Greenville, NC, USA

ARTICLE INFO

Handling Editor: Prof. Jiri Jaromir Klemeš

Keywords:
COVID-19
Nitrile gloves
Expansive soils
Soil stabilisation
Pavement

ABSTRACT

The COVID-19 pandemic not only poses an unprecedented threat to global health but also severely disrupts the natural environment and ecosystems. Mitigating the adverse impacts of plastic-based personal protective equipment (PPE) waste requires the cooperation of professionals from various fields. This paper discusses a novel, cleaner approach to soil stabilisation by repurposing the nitrile gloves into a sustainable road material to improve the mechanical properties of expansive clay soil as pavement subgrade. For the first time, extensive geotechnical testings, including standard compaction, unconfined compressive strength (UCS), unsoaked California bearing ratio (CBR), repeated load triaxial (RLT), and swelling-shrinkage tests, were carried out to investigate the engineering performance of different proportions of the shredded nitrile gloves (SNG) (e.g., 1%, 1.5%, 2%) were blended with expansive clay (EC). In addition, surface roughness, scanning electron microscopy (SEM), and X-ray micro-CT analyses were conducted, and images were obtained to study the microstructural modification of the EC-SNG mixtures. The experimental results indicated that the blend of expansive clay with SNG helped in increasing the compressive strength, resilient modulus, and CBR and assisted in reducing the swelling and shrinkage of the soil. SEM and surface roughness analyses indicated the interaction between the soil matrix interface and the rough surface of the SNG. The main reasons for increasing the strength and stability of clay soil could be attributed to the high tensile strength of the SNG and the formation of the three-dimensional grid, and friction between the soil particles and SNG. According to the X-ray micro-CT test results, the incorporation of SNG led to an increase in closed porosity.

1. Introduction

In accordance with data published by the World Health Organisation (WHO), the COVID-19 pandemic has swept through 237 countries, with nearly 435 million confirmed COVID-19 cases and more than 5.9 million deaths (WHO, 2022). During this highly contagious-novel pandemic, the use of PPE, especially wearing masks and gloves, is essential to achieve the goal of a flat epidemiological curve (Anastopoulos and Pashalidis, 2021; Sangkham, 2020). Ali et al. (2017) stated that approximately 0.5 kg of medical waste per hospital bed daily, including examination gloves, were generated in developed countries, while in developing countries, it is 0.2 kg/bed/day. Sefouhi et al. (2013) found that more than 1100 kg of healthcare wastes, including gloves, were generated every day in the hospital of Batna, Algeria. According to statistical data from Victorian public healthcare services, before the COVID-19 pandemic (in 2010–2011), more than forty thousand tonnes of solid waste, including gloves, were generated by the public healthcare services of the state of Victoria in Australia and only 20% were recycled. The cost to dispose of these wastes was almost $17 million (Department of Health, Victoria, 2021). Prior to the COVID-19 pandemic (in the period 2014–2019), the production of disposable gloves usually had an annual increase of about 6% in Poland. However, since the COVID-19

* Corresponding author.
E-mail addresses: s3557884@student.rmit.edu.au (J. Zhu), mohammad.boroujeni@rmit.edu.au (M. Saberian), Salpadoru.perera@rmit.edu.au (S.T.Anupiya.M. Perera), rajeev.roychand@rmit.edu.au (R. Roychand), jie.li@rmit.edu.au (J. Li), wangg@ecu.edu (G. Wang).
[1] Joint First Author.

https://doi.org/10.1016/j.jclepro.2022.134086
Received 11 April 2022; Received in revised form 29 August 2022; Accepted 9 September 2022
Available online 19 September 2022

outbreak, the production of gloves has increased by 30% in 2020 compared to the same period in 2019 (Jędruchniewicz et al., 2021). Even before the pandemic, gloves were in high demand not only for medical activities but also for other activities such as cleaning, beauty, food and beverage, pharmaceuticals, chemicals, automotive, electronics, construction, laboratories and others (Telugunta et al., 2021). It was estimated that in June 2020, 65 billion gloves were being used each month globally (Prata et al., 2020). Furthermore, WHO estimates that 89 million medical masks, 76 million disposable examination gloves, and 1.6 million pairs of goggles will be required each month globally to prevent the spread of COVID-19 (WHO, 2020). These numbers can be dated back to before the mandatory wearing of PPE was enforced worldwide. Therefore, the global consumption of gloves is estimated to be more than 76 million every month due to the COVID-19 pandemic. The global demand for nitrile gloves is estimated to increase at a compound annual rate of 10.6%–11.2% until 2027 (Patrawoot et al., 2021). In 2021, it was predicted that the market size for nitrile gloves would be worth about 8.76 billion USD. The market for nitrile gloves was evaluated at about 8.76 billion USD in 2021 and was anticipated to increase at an annual rate of 5.7% between 2022 and 2030 (Grand View Research, 2022). Based on the information mentioned above, the gloves will still be in high demand even after the COVID-19 pandemic ends.

Among the various disposable gloves available, nitrile examination gloves and natural rubber latex gloves are widely used in medical applications (Safe Work Australia, 2020). Furthermore, several studies indicated that nitrile medical gloves could be a suitable alternative to latex gloves (Jędruchniewicz et al., 2021). Since the onset of the pandemic, medical facilities and personal protection efforts worldwide have consumed huge amounts of PPE and generated large volumes of medical waste, where face masks and nitrile gloves are the primary sources of these wastes (Ilyas et al., 2020). The indiscriminate use and improper disposal of medical waste have posed a severe threat to the environment and the health of individuals and wildlife (Boroujeni et al., 2021; Sharma et al., 2020). Millions of disposable waste PPE, including gloves, are discarded in parking lots, sidewalks, parks, roadways, and other public places, eventually finding their way to aquatic environments such as puddles, ponds, and lakes (Sarkodie and Owusu, 2021; Wang et al., 2022), leading to the clogging of sewage systems, negatively affecting the infiltration of water, and reducing land productivity to name a few environmental issues (Silva et al., 2021). Plastic waste, including plastic-based waste PPE, scattered in the aquatic environment can become a breeding ground for pests that transmit diseases such as dengue and Zika. The plastic waste eventually makes its way into oceans and other water bodies, where they gradually deteriorate and break up, producing microplastic particles. Microplastic particles are easily ingested by marine animals, causing blockage and permanent damage to their internal organs (Roychand and Pramanik, 2020; Monira et al., 2021). They also pose the risk of entering the human food chain as humans feed on the aforementioned marine life (Kilmartin-Lynch et al., 2021b, 2022). Currently, incineration is known as one of the easiest ways to dispose of medical waste because the high temperature (over 800 degrees Celsius) can destroy pathogens. However, incineration of medical waste is not recommended since large amounts of greenhouse gases and harmful substances such as heavy metals, dioxins, polychlorinated biphenyls, and furans are emitted during this process (Silva et al., 2021). Therefore, based on the explanations mentioned above, it can be reflected that all of this will add to the quantity of waste requiring disposal, adding an additional burden to the environment and public exchequer for its disposal. This waste can be sustainably recycled into strengthening pavement subgrade contributing to increasing the recycling rate of this medical waste material.

Expansive clay soils are widely distributed throughout the earth (Blayi et al., 2020; Steinberg, 2000). Expansive clays vary significantly in volume with changes in moisture content. High compressibility, high potential for expansion and contraction, high plasticity, low permeability, and low shear strength are the distinctive characteristics of these problematic soils (Li et al., 2014). Expansive clays expand dramatically after immersion in water and shrink when they dry out (Khadka et al., 2020). Rainfall, evaporation, and root activity can all trigger changes in the moisture content of expansive soils (Li and Cameron, 2002). Thus, buildings and civil infrastructures on expansive clays often undergo considerable movements due to the soil moisture changes, resulting in displacement, cracking, tilting, or failure. Because of the inferior engineering characteristics of expansive clays, engineering projects such as pavements, railways, and embankments constructed on these poor-quality soils run the risk of premature failure, and they encounter considerable difficulties during construction (Zheng et al., 2009; Sun et al., 2015). Failures of lightly-loaded structures due to the swelling behaviour of expansive soils have been reported worldwide, which lead to severe financial losses and burdens (Zumrawi, 2015). Furthermore, pavements constructed on expansive clays are ten times more expensive to maintain than the same type of roadway built on a non-expansive subgrade (Singh et al., 2016). Chemical stabilisation is commonly used to control the expansive soils on site. Cement and lime are two of the most widely used additives for expansive soil stabilisation (Ghadir et al., 2021). However, cement and lime treatments have a number of inherent disadvantages, such as expensive, carbonation, sulfate attack and environmental concerns due to greenhouse gas emissions. Cement is the source of about 8% of global carbon dioxide (CO_2) emissions. Therefore, a cost-effective and environmentally sustainable alternative is needed to improve the performance of expansive soil (Perera et al., 2022).

There are numerous studies regarding the utilisation of plastic fibres and strips in improving the mechanical properties of problematic soils. It has been indicated that the addition of various kinds of synthetic fibres such as polypropylene (PP), polyethylene terephthalate (PET), and polyvinyl alcohol (PVA) helps in improving the strength, ductility, and other geotechnical properties of soils (Shen et al., 2017; Yarbaşi and Kalkan, 2020). However, to the authors' best knowledge, very limited research has been carried out in pavement geotechnics regarding plastic-based PPE wastes. Saberian et al. (2021a,b) conducted experimental studies on the use of shredded single-use face masks blended with recycled concrete aggregates as road base and subbase. The results showed that the ductility/flexibility of pavement base/subbase improved by introducing the shredded face masks. In addition, the inclusion of the shredded face masks enhanced unconfined compressive strength and resilient modulus because the shredded masks increased the tensile resistance of the mixed samples. According to the research conducted by Rehman and Khalid (2021), both the UCS and CBR of face mask fibre-reinforced fat clay reached the peak value with the introduction of 0.9% face mask fibre. They pointed out that the reasons for the enhancement were the excellent resistance of face mask fibres to fracture and the improved tensile capacity of the soil that resisted deformations. Abdullah and Abd El Aal (2021) evaluated the effect of PPE plastic-based waste on road construction. They found that adding 5% shredded plastic-based PPE waste fragments to the silty sand improved the compressive strength and penetration strength, further revealing that such an improvement was induced by the bridging effect of the PPE waste fragments. Shobana et al. (2021) presented that the inclusion of face masks and banana fibre increased the strength of black cotton soil.

The main aim of this study is to evaluate the technical possibility of using disposable nitrile gloves as a sustainable approach to stabilise and strengthen the expansive clay subgrade. This paper consists of six sections. Section 1 contains the introduction, background of the study and literature review of previous research. Section 2 summarises the significance of the research. Section 3 includes evaluating the geotechnical properties of clay soil and the physical properties of the nitrile glove. Sample preparation and testing methodology are discussed in Section 4. Section 5 provides the testing results, including standard proctor compaction, UCS, CBR, RLT, swelling-shrink, SEM, and X-ray micro-CT tests. Section 6 summarises the main conclusions of this paper and also provides recommendations for future studies.

2. Significance of research

The extensive production and use of PPE have effectively prevented the spread of the virus; however, it has created immense pressure on the environment and landfill sites. To mitigate these issues, the reuse of medical waste in pavement and geotechnical applications is considered a viable solution to reduce the negative environmental impact of the current epidemy (Saberian et al., 2021a,b). Nevertheless, there is a severe lack of knowledge about plastic-based PPE wastes in pavement subgrade applications. In addition, the adoption of nitrile gloves for stabilising expansive soils has never been investigated. Therefore, this study presents a novel and sustainable approach to recycle and reuse nitrile gloves for stabilisation of the expansive clay soil as pavement subgrade. In this study, a comprehensive series of laboratory tests, including compaction, UCS, CBR, RLT, swelling-shrinkage, surface roughness, SEM, and X-ray micro-CT, was conducted to evaluate the feasibility of utilising shredded nitrile gloves (SNG) for stabilisation expansive clay (EC) soil as a pavement construction material. This research would provide valuable insight into the application of disposable nitrile gloves for pavement construction.

3. Materials

3.1. Expansive clay soil

The expansive clay soil was used in this research as the pavement subgrade material. The soil samples were collected from a depth of 1–2 m in a disturbed state from a construction site in Melbourne, Australia. A series of experiments, including particle size distribution (sieve analysis and hydrometer analysis), specific gravity, Atterberg limits, standard proctor compaction test, and swelling-shrinkage tests, were carried out on the expansive clay, following the Australian Standards and ASTM Standards, to obtain the basic geotechnical properties of the soil. The properties are shown in Table 1. The particle size distribution curve for the soil is shown in Fig. 1.

3.2. Shredded nitrile glove

A multi-level, integrated, multi-disciplinary approach is needed to combat COVID-19 and its emerging environmental impact and reduce pandemic-generated waste. Disposable powder-free nitrile gloves were collected and used in this study. The gloves were disinfected and sterilised through isolation and dry heat disinfection. For the isolation process, after a 96-h isolation period (i.e., keeping gloves for at least four days in a sealed container), the used gloves were washed in hot soapy water and finally dried in the sun. Van Doremalen et al. (2020) studied the aerosol and surface stability of SARS-CoV-2, a virus causing COVID-19, and stated that SARS-CoV-2 could survive on plastic and stainless steel for up to 72 h. The isolation procedure was referenced from a study conducted by Kilmartin-Lynch et al. (2021a). After the isolation method was completed, the gloves were oven-dried at 70° for 1 h. The dry heat method is in accordance with a study conducted by Xiang et al. (2020), demonstrating that 1 h of dry heat pasteurisation at 70 °C is sufficient to disinfect and decontaminate used surgical masks. The treated and dried nitrile gloves were then cut into 1 cm wide and 2 cm long strips. The size is the same as previous studies conducted by Castilho et al. (2021), Saberian et al. (2021a,b) and Abdullah and Abd El Aal (2021) on using polyethylene terephthalate strips, face mask strips, and PPE plastic-based waste, respectively, for soil stabilisation and road construction. The physical properties of the SNG used in this research are shown in Table 2. Based on the table, SNG is very light and has a much lower specific gravity than EC. The surface roughness of SNG was examined with Bruker Alicona (IF-Edgemaster) 3D surface analyser. The principle of its operation is to combine the small depth of focus of the optical system with vertical scanning to generate topographical and colour information from changes in focus. As shown in Fig. 2 and D and 3D images of the glove sample (2 cm in length and 1 cm in width) were taken for further geometric analysis. The surface roughness measurement was carried out using software named Alicona-If-measure suite. The roughness of the profile (Ra) of the shredded glove is 4.17 μm, which indicates that the surface of the glove is relatively rough. The roughness of the glove surface helps in increasing the contact area and friction between the shredded glove and the soil particles, thus enhancing the mechanical interlock.

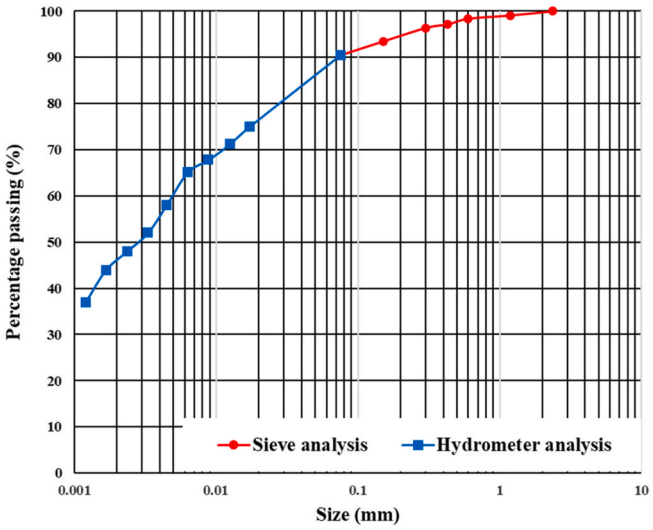

Fig. 1. Particle size distribution curve of expansive clay used in this study.

4. Research methodology

Various mechanical tests were conducted in this study to evaluate the influence of the inclusion of shredded gloves on the geotechnical performance of the expansive clay. Microstructural studies using different microscopy and microanalysis techniques were undertaken to provide a more comprehensive and visual understanding of the expansive soil – shredded gloves mixture. The samples were prepared and tested according to the experimental procedures specified in the relevant standards. The mix design, sample preparations, and test methods are

Table 1
Basic properties of the clay soil.

Properties	Value	Test method
Specific gravity	2.70	ASTM D854-02 (2014)
Optimum moisture content (%)	25	AS 1289.5.1.1 (2017)
Maximum dry density (t/m^3)	1.489	AS 1289.5.1.1 (2017)
Liquid limit (%)	55.87	AS 1289.3.1.1 (2009)
Plastic limit (%)	27.43	AS 1289.3.2.1 (2009)
Plasticity index (%)	28.44	AS 1289.3.3.1 (2009)
Linear shrinkage (%)	6	AS 1289.3.4.1 (2008)
Clay content (%)	65.1	ASTM D422-63 (2007)
Silt content (%)	25.4	ASTM D422–63 (2007)
Sand content (%)	9.5	ASTM D422–63 (2007)
Swell-shrink Index, I_{ss} (%/pF)	3.3	AS 1289.7.1.1 (2003)
Unified soil classification system (USCS)	CH	ASTM D2487-17 (2011)

Table 2
Physical properties of SNG.

Physical properties	Value	Method
Specific gravity	1.25	ASTM D792-20 (2020)
Tensile Strength (MPa)	12.3	ASTM D638-14 (2014)
Elongation at break (%)	240	ASTM D638-14 (2014)
Water absorption 24 h (%)	1.5	ASTM D570-98 (2018)
Melting point (°C)	165	ASTM D7138-16 (2016)
Average roughness of profile (Ra) (μm)	4.17	–

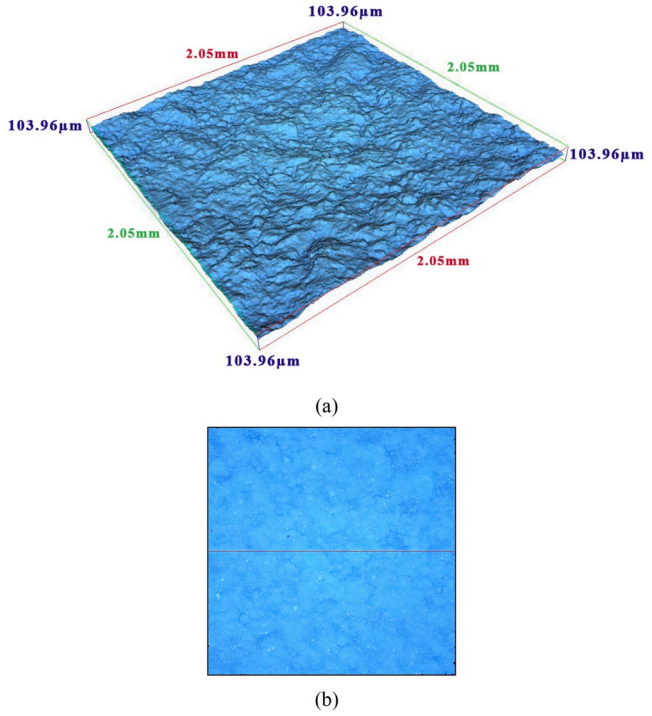

Fig. 2. Images of surface roughness of SNG; (a) 3D image and (b) 2D image.

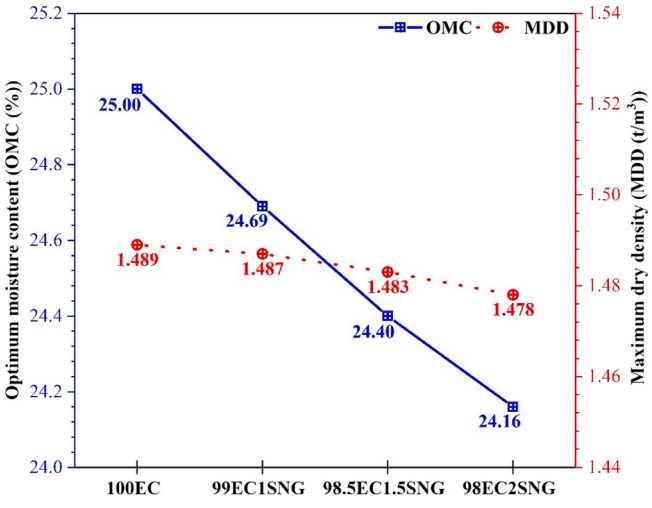

Fig. 3. Test results of standard proctor compaction.

described in this section.

4.1. Preparation of mixtures

For sample preparations, SNG was mixed with oven-dried EC (at 105 °C for 2 days) in three different percentages (1%, 1.5%, and 2% by the dry weight of the soil). This percentage range is consistent with experimental studies conducted by Acharyya et al. (2013), Karmacharya and Acharya (2017), and Soundara (2015) on using waste PET plastic strips and PP plastic fibres for soil stabilisation. The mixtures of EC and SNG were thoroughly blended with water and sealed in plastic bags for five days to allow free water absorption following AS 1289.5.1.1 (2017). Three replicate samples were prepared and tested for each mechanical testing, and the average results were reported. The sample ID for the control clay and three mixtures of EC and SNG used in this study are given in Table 3.

Table 3
The mixtures considered in the laboratory testing programme.

Mix composition	Name of mixtures
100% EC (control clay)	100EC
99% EC + 1% SNG	99EC1SNG
98.5% EC + 1.5% SNG	98.5EC1.5SNG
98% EC + 2.0% SNG	98EC2SNG

4.2. Standard proctor compaction test

In accordance with AS 1289.5.1.1 (2017), standard proctor compaction tests were performed on the four mixtures to measure the maximum dry density (MDD) and optimum moisture content (OMC) of each blend. The oven-dried EC was mixed thoroughly with SNG. Then, various moisture contents were added to each mixture, and the sample was thoroughly blended again until a homogenous mixture was achieved. This mixture was kept in a sealed plastic bag for five days to allow free water absorption and reach an equilibrium state. This curing treatment was also used for sample preparations for UCS, CBR, and RLT tests. The EC-SNG-water mixtures were placed in a mould with a capacity of 1000 cm^3 (UCS mould) and compacted in 3 layers, with each layer receiving 25 blows from the standard compaction hammer. Each layer of the mixture in the mould was compacted by a standard proctor compaction hammer weighing 2.7 kg from a position 300 mm above the top of the layer. The mixtures used for other mechanical tests, i.e., UCS, CBR and RLT tests, were prepared at their relative OMC and MDD.

4.3. Unconfined compressive strength (UCS) test

The unconfined compressive strength test was carried out according to AS 5101.4 (2008). The samples were compacted in three layers in cylindrical metal moulds of 105 mm in diameter and 115.5 mm in height with 25 blows per layer using a standard proctor compaction hammer. The 50 kN Shimadzu Universal Testing machine was used to perform the test with a test speed of 1 mm/min.

4.4. California bearing ratio (CBR) test

The California bearing ratio test was conducted in accordance with AS 1289.6.1.1 (2014). A spacer with a diameter and height of 150 mm and 60 mm, respectively, was placed on the baseplate. The samples were compacted in three layers in a cylindrical metal mould with a diameter of 152 mm and a height of 180 mm, each layer being blown 53 times by using a standard proctor compaction hammer. Testing was carried out on the samples in the CBR moulds with metal surcharge rings weighing 2.25 kg placed on top of the samples using a 50 kN Shimadzu universal testing machine with the plunger attachment set at a 1 mm/min test rate.

4.5. Repeated load triaxial (RLT) test

One of the most significant parameters in designing various pavement layers is the resilient modulus (M_r) (Saberian et al., 2021a,b). M_r can be obtained from the RLT test. Therefore, it is especially critical to determine the behaviour of pavement materials when subjected to stresses from vehicle loading. According to AASHTO designation: AASHTO T 307-99 (2007), the samples were compacted in three layers in a cylindrical metal mould of 100 mm in diameter and 200 mm in height with 40 blows per layer using a standard proctor compaction hammer. The DTS repeated load-triaxial machine was used to apply impulse loading on the samples to simulate the wheel loading from moving vehicles. The samples underwent several loading sequences with different confining stresses and deviatoric stresses applied through repeated cycles for each loading sequence as mentioned in the standard.

4.6. Swelling-shrinkage test

The shrinkage and swell tests are straightforward but important tests commonly used in geotechnical practices to quantitatively evaluate the swelling and shrinkage potentials of remodelled or undisturbed clay soils (Fityus et al., 2005; Li et al., 2016). According to AS 1289.7.1.1 (2003), soil reactivity tests were conducted to determine the shrinkage strain, swell strain, and swell-shrinkage index of the samples. The soil reactivity test consists of two separate tests, the core shrinkage test and the swelling test. Water content has an impact on the swell-shrinkage behaviour of the expansive clays. It is worth mentioning that the expansive soil used in this study had a moisture content of around 22% in its natural state (i.e. at the time of sampling). Therefore, to avoid the impact of water content on the swell and shrinkage tests, the swell-shrinkage samples were prepared at a constant moisture content of 22%. For the core shrinkage test, samples were compacted in three layers in UCS mould using a standard proctor compaction hammer. A 38 mm diameter steel tube was driven into the compacted sample to obtain a cylindrical core shrinkage specimen with a length of between 1.5 and 2 times its diameter. The initial length and mass of the samples were measured and recorded. A metal drawing pin was placed at the centre of each end of the shrinkage samples, and the new mass and the length between the pins were recorded. The samples were then placed on a flat glass plate to allow losing the moisture. The measurements were performed periodically until the shrinkage ceased. Finally, the shrinkage samples were placed in an oven at 105 °C for two days. The final mass and length of the samples were recorded.

The swell samples were compacted in one layer in UCS moulds using a standard proctor compaction hammer. The compacted samples were removed from the mould by using an extruder. A cutting ring of 50 mm in diameter and 19.75 mm in height had been well lubricated with vaseline was driven into each compacted sample to core the swell sample, followed by trimming the surface with a spatula to obtain a flat-surfaced sample. The consolidation cells with cutting rings and samples were assembled. An initial seating load of 5 kPa was applied on the swell test specimen for 10 min, following which a surcharge of 25 kPa was applied for a further 30 min (AS 1289.7.1.1, 2003). The sample was then inundated with distilled water upon the completion of 30 min of applying the 25 kPa surcharge. The samples' response was monitored using the LVDT readings through the software until the variation of LVDT readings that were 3 h apart were less than 5% of total specimen swelling until that time, which was the completion of the test. Once the swelling test was completed, the swelling samples were extracted from the ring, and the final moisture content was determined.

According to AS 1289.7.1.1 (2003), the shrink-swell index I_{SS} can be calculated as:

$$I_{SS} = \frac{\varepsilon_{sh} + \frac{\varepsilon_{sw}}{2.0}}{1.8} \quad (1)$$

where ε_{sh} is the shrinkage strain and ε_{sw} is the swelling strain. There are two empirical parameters in equation (1), a correction factor of 2 for the axial swelling test and an assumed soil suction change range of 1.8 pF (Li et al., 2016).

4.7. Scanning electron microscope (SEM) test

SEM tests were carried out to examine the micro-morphological features of the expansive clay and the reinforced soil with SNG. By analysing the microstructure of the samples, the reasons for improving the mechanical properties of the expansive soil through the addition of SNG can be evaluated. Testing was carried out using an FEI Quanta 200 SEM testing machine on iridium-coated samples. Due to the limitations of the machine, the size of shredded gloves was reduced in equal proportions to a dimension of 2 mm in length and 1 mm in width.

4.8. X-ray micro-CT test

X-ray micro-CT (X-ray micro-tomography) provides data associated with orientation, size, shape, interconnectivity, and distribution of closed pores within the samples. In addition, the distribution of shredded gloves within the compacted soil samples can be visualised. These data and images allow the interpretation of how the incorporation of SNG affects the mechanical properties of expansive soil. Compacted soil samples of 22 mm in height and 26 mm in diameter were mounted in the chamber of the X-ray micro-CT machine (Bruker Skyscan 1275 X-ray micro-tomography (X-ray μCT)). The samples were scanned at 100 kV and 100 mA exposure, creating an axial sequence of X-ray attenuation imagery. A 1 mm copper filter was chosen between the tube and samples to amplify the contrast between the sample phases and reduce the hardening. The 3D image consisted of a voxel size of 10 μm resolution, and data on closed porosity and pore distribution were obtained. It is worth mentioning that the X-ray micro-CT analyses were conducted on the samples of control clay (EC without any SNG) and the EC containing 1.5% SNG, which provided better mechanical results compared to other samples.

5. Results and discussion

5.1. Standard proctor compaction test results

The moisture content-dry density relationships of the various mixtures were demonstrated by conducting the standard proctor compaction test. The variations of the OMC and MDD for the samples with varying percentages of SNG are shown in Fig. 3. The OMC decreased from 25.00% to 24.16% by increasing SNG content from 0 to 2%. The reduction in OMC can be attributed to the low water absorption of the shredded gloves. In addition, by increasing the SNG content from 0 to 2%, MDD decreased slightly from 1.489 t/m^3 to 1.478 t/m^3. The reduction in MDD can be related to the decrease in density of the mixture due to the relatively low density of shredded gloves and the decrease in compaction efficiency resulting from the elastic response of SNG. Kassa et al. (2020) and Ali et al. (2020) observed a similar trend by adding PET strips and PP fibres to the clayey soils, respectively.

5.2. Unconfined compressive strength test results

In pavement geotechnical engineering, one of the most common measurements adopted to investigate the strength of subgrade materials is the unconfined compressive test (MolaAbasi et al., 2020; Saberian and Khabiri, 2017). The UCS test was performed to determine the highest axial stress that the samples could withstand under unconfined pressure conditions and assess the effectiveness of SNG in improving the compressive strength of the EC. The average peak UCS values for the four mixtures with different SNG contents with error bars are given in Fig. 4. By comparing the UCS values of 100EC and 99EC1SNG, it can be observed that the inclusion of 1% of SNG only resulted in a slight increase in compressive strength (from 255.23 kPa to 257.00 kPa). When the SNG addition was increased to 1.5%, the UCS value increased significantly to the peak at 315.50 kPa. The reinforcement mechanism for shredded gloves is comparable to that of rubber fibre reinforcement or plastic strip reinforcement for clay soils. The random and homogeneous mixing of SNG and EC provides a reinforcing result. Combining shredded gloves, having a rough surface, and expansive clay could increase the stretching resistance between the particles. A similar trend was observed in previous studies on the strength properties of clay soils reinforced with plastic (Kassa et al., 2020) and rubber fibres (Yadav and Tiwari, 2017). However, as the SNG content was increased to 2%, the UCS reduced to 297.97 kPa, demonstrating that there is a threshold value of SNG content beyond which the UCS value decreased. Therefore, although the incorporation of SNG contributed to increased strength and integrity of the EC, an excessive introduction of SNG resulted in a

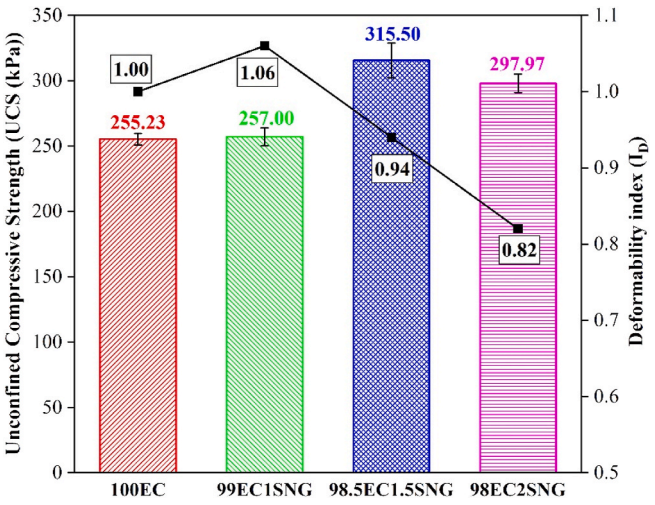

Fig. 4. UCS and deformability index results.

reduction in UCS as the excessive shredded gloves incorporation led to the generation of a high number of voids within the blended sample, thus reducing stiffness. Chen et al. (2015) reported a similar observation in a study on PP fibre reinforced clayey soils. Furthermore, it can be claimed that as the SNG content exceeded 1.5%, the amount of EC matrix available to incorporate the shredded glove was not sufficient to form a binding effectively between EC particles and SNG, which led to the ball of SNG and poor blending. Pradhan et al. (2012) studied the effect of PP fibres on the strength of cohesive soils and noted that incorporating excessive fibres could lead to difficulties in soil compaction, as the fibres would stack and form lumps thereby generating areas of low density.

Fig. 4 also illustrates the variation in the deformation capacity of the control and reinforced samples. The flexibility of the pavement layers is an essential characteristic of flexible pavements (Saberian et al., 2020). According to Jahandari et al. (2021), flexibility (i.e., deformability index) can be evaluated by Equation (3). The equation formulates the deformability index (I_D), which is the ratio of the failure strain of a sample reinforcing with an additive ($\varepsilon_{f\ SNG}$) (SNG in this study) to the failure strain of the control sample ($\varepsilon_{f\ control}$). Based on the deformability index results, the addition of SNG to EC resulted in increasing I_D to the peak 1.06, which could be related to the higher tensile strength and elasticity of the shredded gloves compared to clay particles. This is consistent with previous studies on the geotechnical performance of PP-reinforced expansive soil (Ali et al., 2020). However, the deformability index decreased to 0.94 and 0.82 when the SNG content reached 1.5% and 2%, respectively. The reduced ductility is due to the fact that adding excessive amounts of SNG can lead to difficulties in evenly distributing the SNG inside the sample, resulting in the SNG stacking together.

$$I_D = \varepsilon_{f\ SNG} / \varepsilon_{f\ control} \quad (3)$$

Furthermore, Fig. 5 shows the expansion and deformation of the control clay and reinforced sample (98.5EC1.5SNG) at the failure moment. Fig. 5(a) indicates that the shape of the cylindrical pure soil sample surface can be considered as a flat surface at the moment of failure. However, Fig. 5(b) illustrates that the surface of the soil reinforced with shredded gloves shows a bulging damage pattern at the point of failure, which may be due to deformation caused by blistering within the sample and bar relations. It can be observed that the large cracks that happened in the control clay were replaced by small cracks after incorporating the shredded gloves. Similar surface deformation patterns from the UCS test results were observed in clayey soils stabilised with rubber (Kalkan, 2013), PET (Yarbaşi and Kalkan, 2020), and PP fibres (Zaimoglu and Yetimoglu, 2012). Also, the shredded gloves acted similarly to the root structure of a plant in a way that they connected the fracture surfaces in the sample and distributed the stresses over a wider area, thus effectively preventing further development of cracks and deformation. This is also called the bridging effect (Yarbaşi and Kalkan, 2020).

5.3. California bearing ratio test results

The California bearing ratio (CBR) test is one of the very popular mechanical tests to measure the structural loading bearing capacity of soils for pavement construction (Li et al., 2018). A higher CBR value indicates that the subgrade soil exhibits higher strength, which requires a thinner pavement structure (Abukhettala and Fall 2021). The average CBR test results for four samples with different SNG contents under the

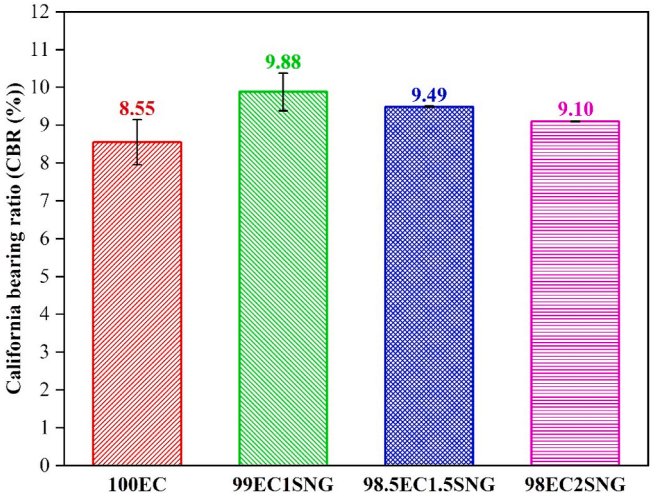

Fig. 6. Effect of SNG on unsoaked CBR.

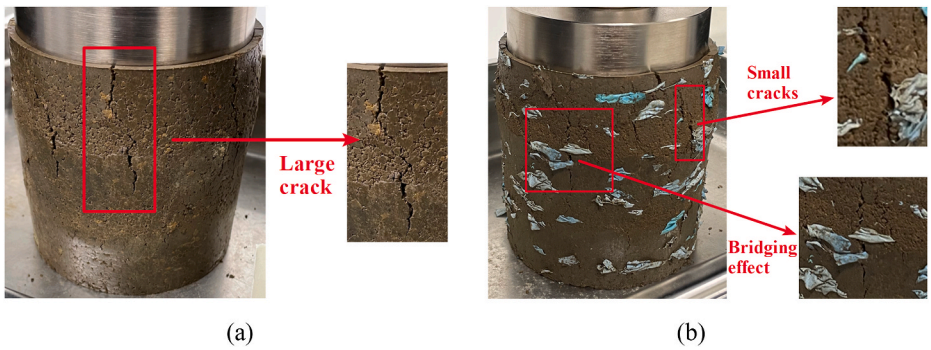

Fig. 5. A view of the surface deformations and failure patterns of the samples at the failure moment in the UCS test; (a) 100EC and (b) 98.5EC1.5SNG.

unsoaked condition with error bars are presented in Fig. 6. It can be observed that the unsoaked CBR values of the expansive soil increased by incorporating 1% SNG. The increase in unsoaked CBR value was because of the rough surface of the shredded gloves contributing to higher internal friction. In addition, the introduction of the bonding material with high tensile strength contributed to enhanced resistance to swelling and improved the resistance to penetration from the plunger. The increase in CBR value proves that the shredded gloves could strengthen the soil particles and provide higher resistance to traffic loads. A similar result for clayey soils reinforced by shredded face masks and PP fibres was presented by Rehman and Khalid (2021) and Tiwari et al. (2020), respectively.

On the other hand, the unsoaked CBR reduced to 9.49% and 9.1% when the shredded gloves were incorporated at 1.5% and 2%, respectively. It is noteworthy that the CBR value of sample 98EC2SNG is still slightly higher than that of the unreinforced sample 100EC. The steady decline in unsoaked CBR values for samples with higher SNG contents (>1%) can be explained by the increased interaction between shredded gloves and the cumulation of these SNG at higher inclusions. A similar trend showing a notable increase and then a gentle decrease in unsoaked CBR values with the addition of rubber fibres was also reported by Yadav and Tiwari (2017).

Hansen (1959) provided design charts for pavement thickness of flexible pavements based on the CBR and traffic volume. Fig. 7(a) shows that the required subgrade thicknesses for the control clay are approximately 262 mm, 291 mm, 312 mm for light, medium, and heavy traffic volumes, respectively, based on its CBR value of 8.55%. Under the light, medium, and heavy traffic conditions, the required subgrade thicknesses can be reduced to approximately 241 mm, 268 mm, and 288 mm, respectively, for the sample containing 1% SNG having a CBR value of 9.88% (Fig. 7(b)). This means that adding 1% of SNG reduces the subgrade thickness by about 8%, which can be translated to the reduction in pavement construction costs as well as proposing a cleaner and sustainable road infrastructure.

5.4. Repeated load triaxial test results

The resilient modulus (M_r) is a typical indicator to characterise unbound granular materials and subgrade soils. It demonstrates the dynamic properties and load-bearing capacity of the pavement material under cyclic traffic loadings (El-Badawy and Valentin, 2018). The resilient modulus results for the four mixtures containing different SNG contents are presented in Fig. 8. The M_r values are the average of the resilient modulus values from the 15 stages of the RLT tests. Based on the results, by increasing the SNG content from 0 to 1.5%, M_r increased from 56.61 MPa to 79.98 MPa. The increase in M_r can be explained by the fact that shredded gloves with rough surfaces could enhance stretching resistance, inter-particle tensile resistance, and internal friction between the clay particles. However, a further increase in SNG content resulted in a reduction in M_r value. The decrease in resilient modulus can be attributed to the high incorporation of SNG, resulting in the generation of many voids and entanglement of shredded gloves, as well as the introduction of a large number of low-density zones, which negatively impacted the bonding between soil particles and SNG. El-Badawy and Valentin (2018) investigated the effect of recycled PET strips as soil reinforcement on the resilient modulus of low plasticity soil and found similar results. Also, the results of Saberian et al. (2021a,b) on the adoption of shredded face masks for reinforcing recycled concrete aggregate for the construction of pavement base and subbase provided similar results.

Fig. 9 depicts the variation of average M_r values of the samples versus the number of stress stages of the RLT test. According to AASHTO T 307-99 (2007), the inputs for the confining stress of the RLT tests decrease from 41.4 kPa to 13.8 kPa for clay subgrades. Therefore, a comparison between the test inputs recommended by the standard and the results from Fig. 9 indicates that the resilient modulus was reduced

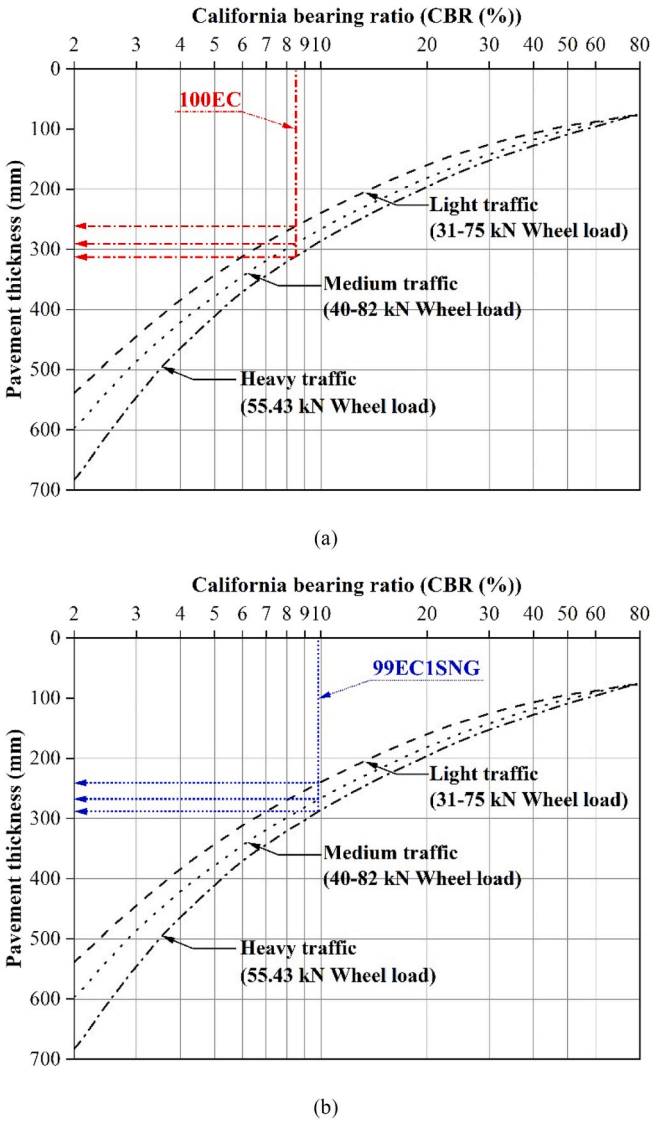

Fig. 7. CBR *vs* flexible pavement thickness curves for (a) control clay and (b) 99EC1SNG.

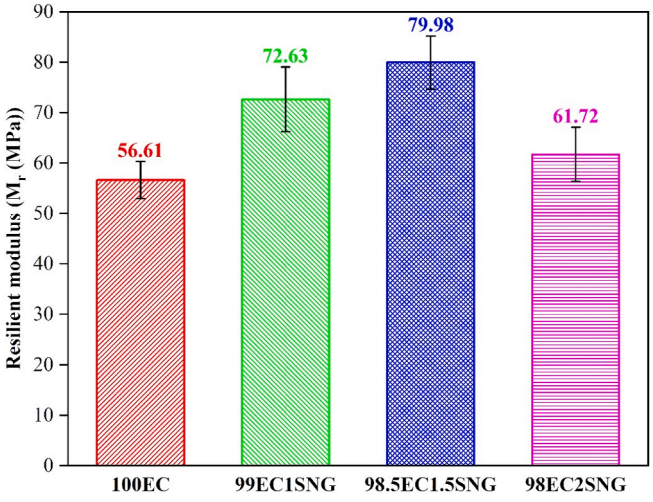

Fig. 8. Effect of SNG on resilient modulus.

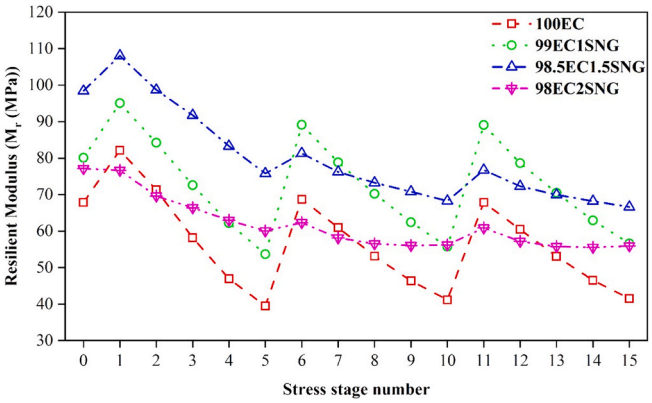

Fig. 9. Variation of average M_r values of the samples versus the number of stress stages.

by decreasing confining stress. This can be attributed to the reason that the clay subgrade has a tendency to get denser by the reduction in the voids as confinement increases, which causes an increase in stiffness. In this case, the clay subgrade experiences a lower recoverable deformation, causing a higher M_r. Furthermore, at a constant confining stress (σ_3) and under varying deviator stress (σ_d), M_r was increased by increasing the deviator stress.

Several models have been proposed to predict/model the M_r of clay subgrades through the RLT test results. In this study, two models of (a) the deviatoric stress model (Equation (4)), proposed by AASHTO T 294-94 (1994), and (b) Pezo's model (Pezo, 1993) (Equation (5)) were used for modelling the M_r of the samples. As can be seen from Equation (4), the M_r relates to the deviatoric stress (σ_d), but this model oversimplifies the M_r behaviour of soils since it does not consider the effect of confining stress (σ_3). Therefore, Pezo's model, which relates M_r to the combination of σ_d and σ_3, was also adopted in this research.

$$M_r = k_1\,\sigma_d\,^{\frac{k}{2}} \tag{4}$$

$$M_r\cdot = \cdot K_3\cdot P_a\cdot\left(\frac{\sigma_3}{P_a}\right)^{k_4}\left(\frac{\sigma_d}{P_a}\right)^{k_5} \tag{5}$$

where k_1-k_5 are the regression parameters, and P_a is the atmospheric pressure.

The regression parameters of the deviatoric stress model and Pezo's model, and the coefficient of determination (R^2) values of the samples are provided in Table 4.

It can be implied from the results of Table 4 that the three-parameter model (Pezo's model) could model the M_r of the samples with higher accuracy than the deviatoric stress model as the R^2 values obtained from Pezo's model vary from 0.70 to 0.93, while the R^2 values of the deviatoric stress model are in the range of 0.26–0.92. Another result is that the k_2 constants, which relate to σ_d, of both models had negative values. Thus, it can be inferred that M_r decreases as the σ_d increases. Fig. 10 shows that Pezo's model could provide an excellent fit ($R^2 = 0.91$) and a linear trend between the predicted M_r and experimental measured M_r of the samples. However, the fit was moderately good for the deviatoric stress model ($R^2 = 0.78$).

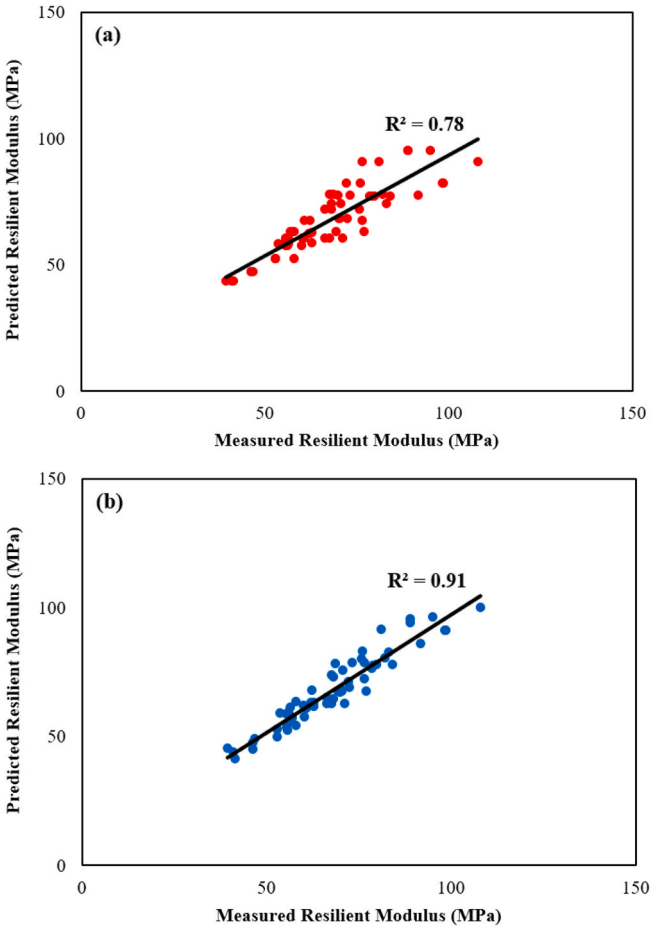

Fig. 10. Relationships between the measured M_r and modelled M_r by (a) deviatoric stress model and (b) Pezo's model.

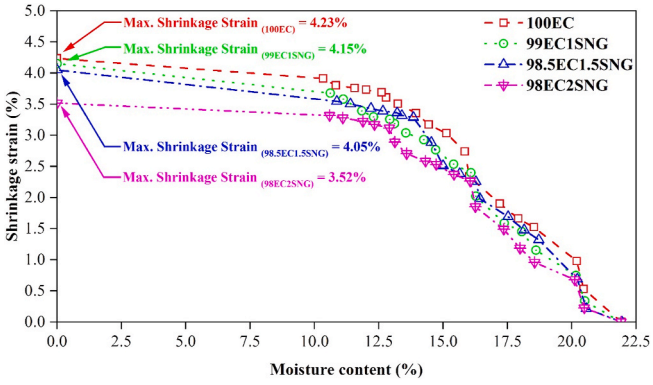

Fig. 11. Axial shrinkage strain versus moisture content.

Table 4
The regression parameters of the clay samples obtained from the deviatoric stress model and Pezo's model.

Sample	Deviatoric stress model			Pezo's model			
	K_1	K_2	R^2	K_3	K_4	K_5	R^2
100EC	195.842	−0.364	0.82	0.407	0.079	−0.363	0.87
99EC1SNG	206.664	−0.306	0.92	0.519	0.019	−0.306	0.93
98.5EC1.5SNG	131.004	−0.145	0.29	0.913	0.223	−0.140	0.80
98EC2SNG	87.423	−0.102	0.26	0.675	0.153	−0.098	0.70

5.5. Swelling-shrinkage test results

The shrinkage and swelling test results are presented in Figs. 11–13. Fig. 11 shows the effect of different SNG contents on the shrinkage strain of the expansive clay. It can be observed from Fig. 11 that the maximum shrinkage strain of expansive clay decreased from 4.23% to 3.52% by increasing the SNG content from 0 to 2%. Furthermore, Fig. 12 illustrates the effect of different SNG contents on the swelling strain of the expansive clay. As can be seen, the maximum swelling strain of the expansive clay decreased from 3.27% to 1.36% when the SNG content increased from 0% to 2%. It should be noted that at the beginning of the swelling test, the swelling strain of 100EC was higher than that of 99EC1SNG; however, at the end of the experiment, the maximum swelling strains for both 100EC and 99EC1SNG were 3.27% and 3.26%, which are very similar. This could be due to the lack of enough SNG to effectively reduce the swelling shrinkage potential at 1% inclusion. Therefore, the clay-clay interaction was still dominant instead of the more desirable EC-SNG interaction. Fig. 13 presents the results of the shrink-swell index of the four mixtures. As seen from the figure, when SNG contents increased to 2%, the shrink-swell index of the blends decreased from 3.26%/pF to 2.33%/pF. The reasons for the decrease in shrinkage strain, swelling strain, and shrink-swell index of expansive clays with the addition of shredded gloves are (i) part of the expansive soil was replaced by shredded gloves that did not swell, which certainly reduced the expansion and contraction capacity, (ii) the SNG improved frictional resistance against movements during swelling and shrinkage, (iii) the randomly dispersed SNG in the soil mixtures formed a 3-D grid structure, thus limiting the movement of the expansive clay particles during swelling and shrinking, and (iv) swelling-shrinkage posed tensile stress/strain since gloves had relatively good tensile performance, they could hold the clay particles in place by resisting these tensile forces.

5.6. Scanning electron microscope test results

Figs. 14 and 15 show the SEM images of the control sample (EC only) and clay soil reinforced with 1.5% SNG at different magnification levels, respectively. From Fig. 14, it can be seen that there are many pores in the pure soil sample. As the sample is subjected to loading, the soil particles tend to slide, leading to cracks and deformations and subsequently low strength. When the water content increases, the voids can facilitate the penetration and movement of water, and clay particles absorb large amounts of water, which causes the swelling of the expansive clay. As can be seen from Fig. 15, several clay particles are attached to the surface of the shredded gloves, which shows the good bonding performance of SNG with the clay particles. In addition, it can be clearly seen that the shredded gloves have a rough surface texture, which also contributes to mechanical interlocking with compacted clay, thereby improving the strength properties. Tang et al. (2007) noted similar observations of the roughness of polypropylene fibres improving the sliding resistance and bond strength of clay soil. In addition, the randomly dispersed shredded

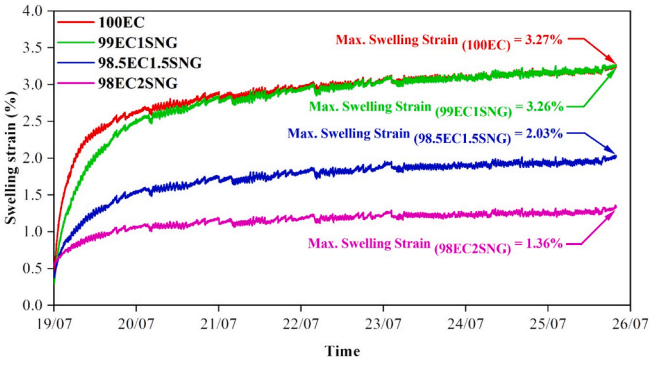

Fig. 12. Swelling strain versus time.

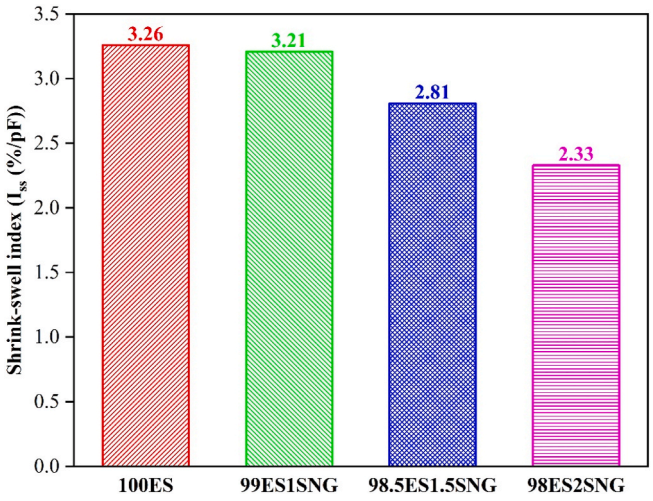

Fig. 13. Test results of the swelling-shrinkage test.

gloves in the soil matrix form a three-dimensional network structure that allows the EC and SNG to interlock and form a stable structure, thus limiting the displacement of soil particles from one position to another. In this way, the swelling behaviour of the expansive soil is limited, and its strength is increased.

5.7. X-ray micro-CT test results

As mentioned previously, the porosity affects the geotechnical properties of soils. Therefore, to study this phenomenon, X-ray micro-CT experiments were conducted to investigate the distribution of closed pores and closed porosity of the control sample and compacted clay containing 1.5% SNG.

A total of 1347 2D images of cylindrical soil samples of 26 mm in diameter and 22 mm in height with a 25 μm thickness were obtained. The 2D micro-CT scanning images illustrate the abundance, shape, distribution, and size of the macropores and micropores at specific sections of the soil sample. Fig. 16 shows the 2D image slice of the random section selected from the compacted control clay sample. In the 2D image, the white and light grey areas represent the soil particles, while the black areas represent the micropores.

3D numerical simulations were carried out using two-dimensional images to investigate the three-dimensional structural characteristics of the closed pores within the soil samples, including shape, interconnectivity, and distribution. Fig. 17 illustrates the 3D X-ray micro-CT scanning images of the compacted expansive soil sample and the compacted sample containing 1.5% SNG. Also, Table 5 provides the closed porosity values of the compacted 100EC and 98.5EC1.5SNG samples. As shown in Fig. 17(a), the closed pores in the control clay are evenly dispersed throughout the sample, and the number of pores is relatively less. However, more closed pores can be observed in the sample mixed with 1.5% SNG (Fig. 17(b)) that concentrated in the middle of the sample, resulting in larger voids and increased porosity. The inclusion of 1.5% SNG increased the closed porosity from 1.003% (i.e., closed porosity of control clay) to 2.404%. The reasons for the increase in closed porosity with the incorporation of shredded gloves are (i) the elastic behaviour of the SNG led to poor compaction and (ii) SNG stacked up and formed lumps, leading to the formation of low-density regions.

Fig. 18 shows a 3-D image of the distribution of the 1.5% SNG in the compacted sample. It can be clearly seen that the shredded gloves are relatively evenly distributed in the sample. However, after compacting, the SNG overlaps and forms irregular shapes. As the surface of the SNG is not cohesive, the overlapping of the SNG results in gaps between the gloves and the formation of low-density areas, which are responsible for

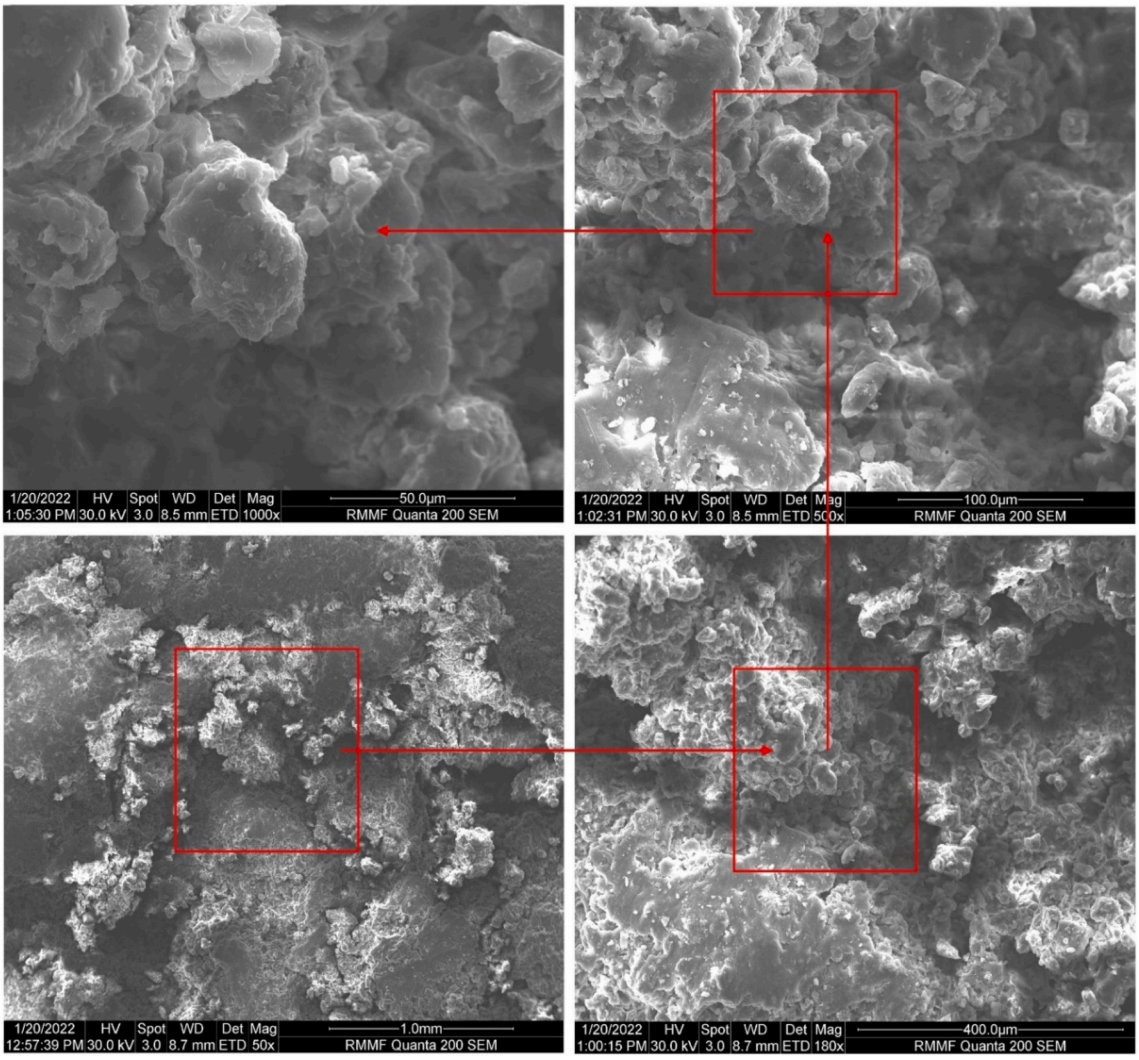

Fig. 14. SEM images of control EC.

the increase in closed porosity.

6. Conclusions and recommendations for future studies

This research proposes an innovative and sustainable methodology to mitigate pandemic-generated waste by recycling disposable nitrile rubber gloves in subgrade layers of pavement. The following conclusions can be derived from the experimental results of this research.

- By increasing the SNG content, the OMC and MDD decreased. The decrease in OMC was attributed to the low water absorption of SNG, and the decline in MDD was due to the lower specific gravity of SNG compared to EC.
- The addition of 1% SNG led to an improvement in the ductility and flexibility of the EC-SNG mixture because of the higher tensile strength of SNG. However, higher inclusions of SNG reduced the ductility and flexibility, as shredded gloves stacked on top of each other.
- The introduction of 1–1.5% SNG to EC led to an increase in strength and stiffness of the mixtures in terms of the UCS, which was because SNG enhanced the bonding of EC particles and the bridging effect of the SNG in the mixtures prevented the development of further tensile cracks. However, as the SNG addition exceeded 1.5%, the strength and stiffness of the EC-SNG mixture decreased due to the stacking of SNG caused by the excess incorporation, resulting in a large number of gaps within the sample.
- It was observed that the inclusion of SNG led to an increase in the unsoaked CBR. This was attributed to the rough surface of the glove contributing to higher internal friction, as well as its high tensile strength, causing an increase in the resistance to plunger penetration. The inclusion of SNG contributed to the higher load-bearing capacity of the pavement subgrade, which directly led to a reduction in subgrade thickness and savings in construction costs and time.
- With the addition of 1.5% SNG, M_r increased to the peak at 79.98 MPa and then decreased by higher inclusion of SNG. The increase was attributed to the shredded gloves with rough surfaces that could enhance stretching resistance, inter-particle tensile resistance, and internal friction between the clay particles.
- The shrinkage strain, swelling strain, and shrinkage-swelling index decreased with increasing the SNG content, indicating that the shredded gloves could effectively reduce the shrinkage-swelling behaviour of the expansive clay.
- The SEM analysis showed that SNG had difficulty sliding in the soil matrix because of the increased friction caused by the grooves and pits on the surface of the gloves. Also, the SNG in the soil matrix formed a three-dimensional network structure that allowed the EC and SNG to interlock and create a stable and uniform system, thus limiting the displacement of soil particles from one position to another.

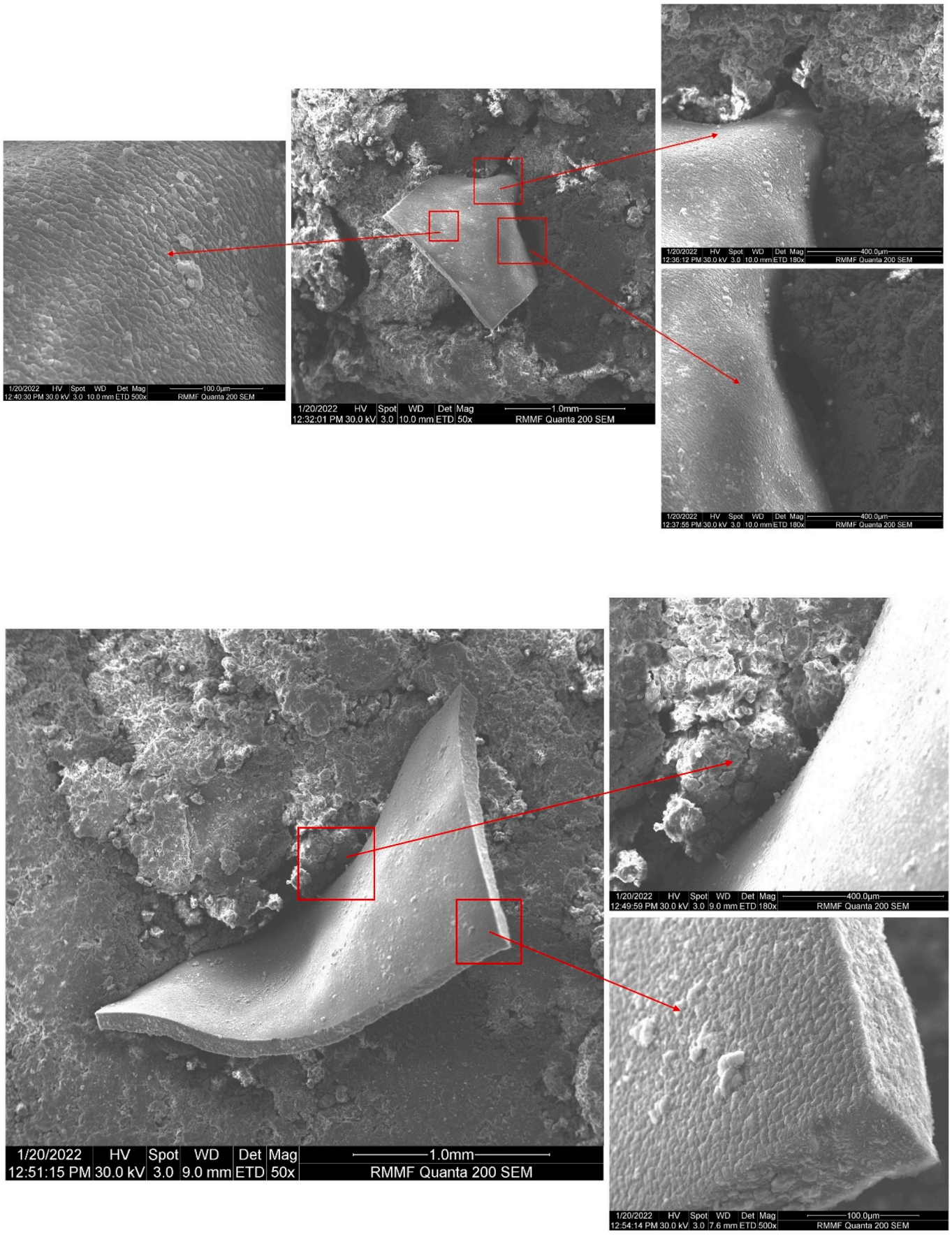

Fig. 15. SEM images of EC reinforced with 1.5% SNG.

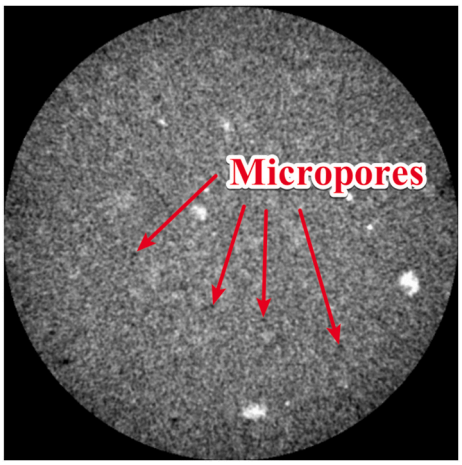

Fig. 16. 2D Micro-CT scanning image of the compacted sample of 100EC

- According to the X-ray micro-CT results, the addition of SNG resulted in an increase in closed porosity due to the elastic behaviour of SNG, causing poor compaction, as well as stacking up the SNG, forming lumps and leading to the formation of low-density regions.
- In general, EC-SNG mixtures can provide a sustainable solution for PPE waste management generated by the pandemic and enhance the strength and stability of the expansive clay subgrade. Thus, shredded nitrile gloves are deemed to be a promising alternative to subgrade materials.
- For the construction of 1 km of a road subgrade with a width of 3.5m and depth of 0.3m, approximately 23 tonnes of nitrile gloves are required, i.e. preventing approximately 4.75 million used nitrile gloves from ending up in landfills. This can lead to moving toward sustainability and the circularity of road construction.

Considering that the majority of PPE wastes are plastic-based, including polypropylene, vinyl, latex, and nitrile, the presented testing methodology could be adapted to different PPE. Feasibility studies similar to the one reported here are required to be performed to investigate the potential application of other PPE wastes, such as disposable gowns, PVC gloves, latex gloves, and non-woven masks, for the stabilisation of expansive clay soils. In future research, the effect of different sizes of shredded nitrile gloves on the geotechnical properties of the expansive clay soils can be considered. Also, future studies can consider other SNG contents as a recommendation lower than 1% (i.e., 0.1%, 0.03%, 0.5%, 0.7% and 0.9%).

CRediT authorship contribution statement

Jiasheng Zhu: Methodology, Validation, Investigation, Writing – original draft, Data curation, Formal analysis, Visualization. **Mohammad Saberian:** Methodology, Validation, Investigation, Writing – review & editing, Data curation, Formal analysis, Visualization. **Salpadoru Tholkamudalige Anupiya. M. Perera:** Methodology, Validation, Investigation, Writing – review & editing, Data curation, Formal analysis, Visualization. **Rajeev Roychand:** Investigation, Writing – review & editing, Data curation, Formal analysis, Visualization. **Jie Li:** Conceptualization, Writing – review & editing, Resources, Validation, Supervision, Project administration, Formal analysis, Visualization. **George Wang:** Writing – review & editing, Supervision, Visualization.

Declaration of competing interest

The authors declare that they have no known competing financial

Table 5
Closed porosity values of the 100EC and 98.5EC1.5SNG samples.

Samples	100EC	98.5EC1.5SNG
Closed porosity (%)	1.003	2.404

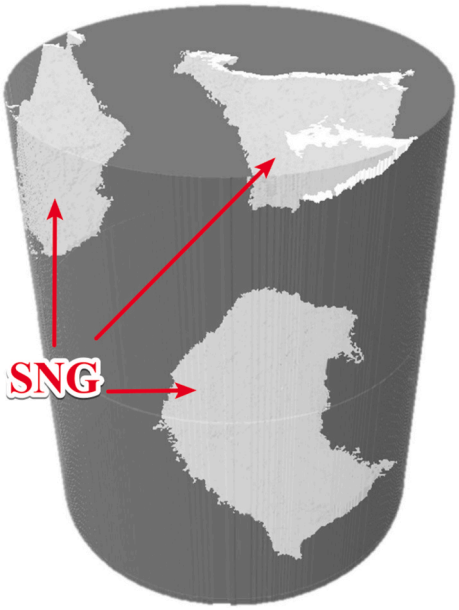

Fig. 18. Distribution of 1.5% SNG in EC.

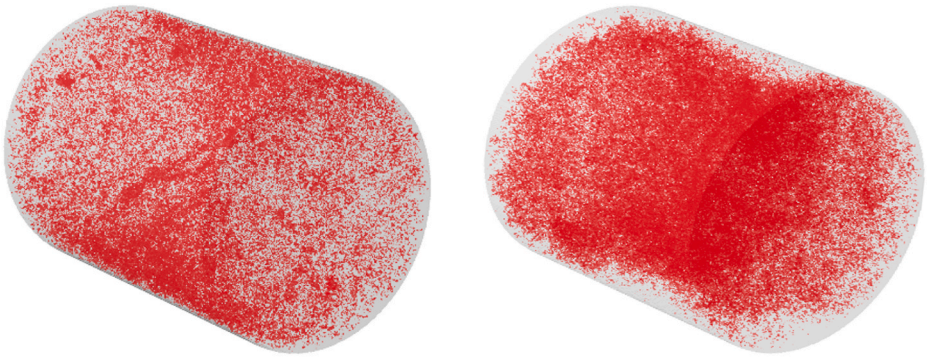

Fig. 17. 3D micro-CT scanning images of the compacted samples of (a) 100EC and (b) 98.5EC1.5SNG.

interests or personal relationships that could have appeared to influence the work reported in this paper.

Data availability

Data will be made available on request.

Acknowledgments

This research was supported by A & Y Associates and a **veski** fellowship to MS. The authors gratefully acknowledge the RMIT Microscopy and Microanalysis Facility for providing training and access to the facility.

References

AASHTO T 294-94, 1994. Standard Test Method of Tests for Resilient Modulus of Subgrade Soils and Untreated Base/subbase Materials. AASHTO T 294-94, Washington, DC.
AASHTO T 307-99, 2007. Standard Method of Test for Determining the Resilient Modulus of Soils and Aggregate Materials. AASHTO T307-99, Washington, DC.
Abdullah, G.M., Abd El Aal, A., 2021. Assessment of the reuse of Covid-19 healthy personal protective materials in enhancing geotechnical properties of Najran's soil for road construction: numerical and experimental study. J. Clean. Prod. 320, 128772.
Abukhettala, M., Fall, M., 2021. Geotechnical characterisation of plastic waste materials in pavement subgrade applications. Transport. Geotech. 27, 100472.
Acharyya, R., Lahiri, A., Mukherjee, S.P., Raghu, P.V., 2013. Improvement of undrained shear strength of clayey soil with PET bottle strips. In: Proceedings of Indian Geotechnical Conference December.
Ali, M., Aziz, M., Hamza, M., Madni, M.F., 2020. Engineering properties of expansive soil treated with polypropylene fibres. Geomech. Eng. 22 (3), 227–236.
Ali, M., Wang, W., Chaudhry, N., Geng, Y., 2017. Hospital waste management in developing countries: a mini review. Waste Manag. Res. 35 (6), 581–592.
Anastopoulos, I., Pashalidis, I., 2021. Single-use surgical face masks, as a potential source of microplastics: do they act as pollutant carriers? J. Mol. Liq. 326, 115247.
AS 1289.3.1.1, 2009. Methods of Testing Soils for Engineering Purposes, Method 3.1.1: Soil Classification Tests - Determination of the Liquid Limit of a Soil - Four Point Casagrande Method. Australian Standard, Sydney, NSW, Australia, pp. 1–13. Australian Standard 1289.3.1.1.
AS 1289.3.2.1, 2009. Methods of Testing Soils for Engineering Purposes, Method 3.2.1: Soil Classification Tests - Determination of the Plastic Limit of a Soil - Standard Method. Australian Standard, Sydney, NSW, Australia, pp. 1–4. Australian Standard 1289.3.2.1.
AS 1289.3.3.1, 2009. Methods of Testing Soils for Engineering Purposes, Method 3.3.1: Soil Classification Tests - Calculation of the Plasticity Index of a Soil. Australian Standard, Sydney, NSW, Australia, pp. 1–4. Australian Standard 1289.3.3.1.
AS 1289.3.4.1, 2008. Methods of Testing Soils for Engineering Purposes, Method 3.4.1: Soil Classification Tests - Determination of the Linear Shrinkage of a Soil-Standard Method. Australian Standard, Sydney, NSW, Australia, pp. 1–3. Australian Standard 1289.3.4.1.
AS 1289.5.1.1, 2017. Methods of Testing Soils for Engineering Purposes, Method 5.1.1: Soil Compaction and Density Tests - Determination of the Dry Density/Moisture Content Relation of a Soil Using Standard Compactive Effort. Australian Standard, Sydney, NSW, Australia, pp. 1–13. Australian Standard 1289.5.1.1.
AS 1289.6.1.1, 2014. Methods of Testing Soils for Engineering Purposes, Method 6.1.1: Soil Strength and Consolidation Tests - Determination of the California Bearing Ratio of a Soil - Standard Laboratory Method for a Remoulded Specimen. Australian Standard, Sydney, NSW, Australia, pp. 1–24. Australian Standard 1289.6.1.1.
AS 1289.7.1.1, 2003. Methods of Testing Soils for Engineering Purposes, Method 7.1.1: Soil Reactivity Tests - Determination of the Shrinkage Index of a Soil-Shrink-Swell Index. Australian Standard, Sydney, NSW, Australia, pp. 1–8. Australian Standard 1289.7.1.1.
AS 5101.4, 2008. Methods for Preparation and Testing of Stabilized Materials. Method 4: Unconfined Compressive Strength of Compacted Materials. Australian Standard 5101.4. Australian Standard, Sydney, NSW, Australia, pp. 1–12.
ASTM D854-02, 2014. Standard Test Methods for Specific Gravity of Soil Solids by Water Pycnometer. Annual Book of ASTM Standards. American Society for Testing and Materials, West Conshohocken, PA.
ASTM D2487-17, 2011. Standard Practice for Classification of Soils for Engineering Purposes (Unified Soil Classification System). Annual Book of ASTM Standards, West Conshohocken, PA.
ASTM D422–63, 2007. Standard Test Method for Particle-Size Analysis of Soils. Annual Book of ASTM Standards, West Conshohocken, PA. ASTM Standard Test Method, D422-63.
ASTM D570-98, 2018. Standard Test Method for Water Absorption of Plastics. Annual Book of ASTM Standards, West Conshohocken, PA.
ASTM D638-14, 2014. Standard Test Method for Tensile Properties of Plastics. Annual Book of ASTM Standards, West Conshohocken, PA.
ASTM D7138-16, 2016. Standard Test Method to Determine Melting Temperature of Synthetic Fibres. Annual Book of ASTM Standards, West Conshohocken, PA.
ASTM D792-20, 2020. Standard Test Methods for Density and Specific Gravity (Relative Density) of Plastics by Displacement. Annual Book of ASTM Standards, West Conshohocken, PA.
Blayi, R.A., Sherwani, A.F.H., Ibrahim, H.H., Faraj, R.H., Daraei, A., 2020. Strength improvement of expansive soil by utilising waste glass powder. Case Stud. Constr. Mater. 13, e00427.
Boroujeni, M., Saberian, M., Li, J., 2021. Environmental impacts of COVID-19 on Victoria, Australia, witnessed two waves of Coronavirus. Environ. Sci. Pollut. Control Ser. 28 (11), 14182–14191.
Castilho, T.W., Rodrigues, R.A., Lodi, P.C., 2021. Use of recycled polyethylene terephthalate strips in soil improvement. Geotech. Geol. Eng. 39 (8), 5943–5955.
Chen, M., Shen, S.L., Arulrajah, A., Wu, H.N., Hou, D.W., Xu, Y.S., 2015. Laboratory evaluation on the effectiveness of polypropylene fibres on the strength of fibre-reinforced and cement-stabilised Shanghai soft clay. Geotext. Geomembranes 43 (6), 515–523.
Department of Health, Victoria. (2021). Waste. https://www.health.vic.gov.au/planning-infrastructure/waste. Viewed on 28th July 2022..
El-Badawy, S., Valentin, J. (Eds.), 2018. Sustainable Solutions for Railways and Transportation Engineering. Proceedings of the 2nd GeoMEast International Congress and Exhibition on Sustainable Civil Infrastructures, Egypt 2018–The Official International Congress of the Soil-Structure Interaction Group in Egypt (SSIGE). Springer.
Fityus, S.G., Cameron, D.A., Walsh, P.F., 2005. The shrink swell test. Geotech. Test J. 28 (1), 92–101.
Ghadir, P., Zamanian, M., Mahbubi-Motlagh, N., Saberian, M., Li, J., Ranjbar, N., 2021. Shear strength and life cycle assessment of volcanic ash-based geopolymer and cement stabilized soil: a comparative study. Transport. Geotech. 31, 100639.
Grand View Research, 2022. Nitrile Gloves Market Size, Share & Trends Analysis Report by Type (Powder Free, Powdered), by Product (Disposable, Durable), by End Use (Medical & Healthcare), by Region, and Segment Forecasts, 2022 – 2030. Grand View Research. July 07, 2022. https://www.grandviewresearch.com/industry-analysis/nitrile-gloves-market.
Hansen, J.B., 1959. Developing a Set of CBR Curves. U.S. *Army Corps of Engineers*. Instruction Report No. 4.
Ilyas, S., Srivastava, R.R., Kim, H., 2020. Disinfection technology and strategies for COVID-19 hospital and bio-medical waste management. Sci. Total Environ. 749, 141652.
Jahandari, S., Tao, Z., Saberian, M., Shariati, M., Li, J., Abolhasani, M., Kazemi, M., Rahmani, A., Rashidi, M., 2021. Geotechnical properties of lime-geogrid improved clayey subgrade under various moisture conditions. Road Mater. Pavement Des. 1–19.
Jędruchniewicz, K., Ok, Y.S., Oleszczuk, P., 2021. COVID-19 discarded disposable gloves as a source and a vector of pollutants in the environment. J. Hazard Mater. 417, 125938.
Kalkan, E., 2013. Preparation of scrap tire rubber fibre–silica fume mixtures for modification of clayey soils. Appl. Clay Sci. 80, 117–125.
Karmacharya, R., Acharya, I.P., 2017. Reinforcement of soil using recycled polyethylene terephthalate (PET) bottle strips. In: Proceedings of IOE Graduate Conference, vol. 5, pp. 153–156.
Kassa, R.B., Workie, T., Abdela, A., Fekade, M., Saleh, M., Dejene, Y., 2020. Soil stabilisation using waste plastic materials. Open J. Civ. Eng. 10 (1), 55–68.
Khadka, S.D., Jayawickrama, P.W., Senadheera, S., Segvic, B., 2020. Stabilisation of highly expansive soils containing sulfate using metakaolin and fly ash based geopolymer modified with lime and gypsum. Transport. Geotech. 23, 100327.
Kilmartin-Lynch, S., Roychand, R., Saberian, M., Li, J., Zhang, G., 2021a. Application of COVID-19 Single-Use Shredded Nitrile Gloves in Structural Concrete: Case Study from Australia. Science of The Total Environment, 151423.
Kilmartin-Lynch, S., Saberian, M., Li, J., Roychand, R., Zhang, G., 2021b. Preliminary evaluation of the feasibility of using polypropylene fibres from COVID-19 single-use face masks to improve the mechanical properties of concrete. J. Clean. Prod. 296, 126460.
Kilmartin-Lynch, S., Roychand, R., Saberian, M., Li, J., Zhang, G., Setunge, S., 2022. A sustainable approach on the utilisation of COVID-19 plastic based isolation gowns in structural concrete. Case Stud. Constr. Mater. 17, e01408.
Li, J., Cameron, D.A., 2002. Case study of courtyard house damaged by expansive soils. J. Perform. Constr. Facil. 16 (4), 169–175.
Li, J., Cameron, D.A., Ren, G., 2014. Case study and back analysis of a residential building damaged by expansive soils. Comput. Geotech. 56, 89–99.
Li, J., Saberian, M., Nguyen, B.T., 2018. Effect of crumb rubber on the mechanical properties of crushed recycled pavement materials. J. Environ. Manag. 218, 291–299.
Li, J., Zou, J., Bayetto, P., Barker, N., 2016. Shrink-swell index database for Melbourne. Aust. Geomech J. 51 (3).
MolaAbasi, H., Semsani, S.N., Saberian, M., Khajeh, A., Li, J., Harandi, M., 2020. Evaluation of the long-term performance of stabilised sandy soil using binary mixtures: a micro-and macro-level approach. J. Clean. Prod. 267, 122209.
Monira, S., Bhuiyan, M.A., Haque, N., Shah, K., Roychand, R., Hai, F.I., Pramanik, B.K., 2021. Understanding the fate and control of road dust-associated microplastics in stormwater. Process Saf. Environ. Protect. 152, 47–57.
Patrawoot, S., Tran, T., Arunchaiya, M., Somsongkul, V., Chisti, Y., Hansupalak, N., 2021. Environmental impacts of examination gloves made of natural rubber and nitrile rubber, identified by life-cycle assessment. SPE Polymers 2 (3), 179–190.
Perera, M.S.T.A., Saberian, M., Zhu, J., Roychand, R., Li, J., 2022. Effect of crushed glass on the mechanical and microstructural behavior of highly expansive clay subgrade. Case Stud. Constr. Mater. 17, e01244.

Pezo, R.F., 1993. A general method of reporting resilient modulus tests of soils, a pavement engineer's point of view. In: 72nd Annual Meeting of the TRB.
Pradhan, P.K., Kar, R.K., Naik, A., 2012. Effect of random inclusion of polypropylene fibres on strength characteristics of cohesive soil. Geotech. Geol. Eng. 30 (1), 15–25.
Prata, J.C., Silva, A.L., Walker, T.R., Duarte, A.C., Rocha-Santos, T., 2020. COVID-19 pandemic repercussions on the use and management of plastics. Environ. Sci. Technol. 54 (13), 7760–7765.
Rehman, U.Z., Khalid, U., 2021. Reuse of COVID-19 face mask for the amelioration of mechanical properties of fat clay: a novel solution to an emerging waste problem. Sci. Total Environ. 794, 148746.
Roychand, R., Pramanik, B.K., 2020. Identification of micro-plastics in Australian road dust. J. Environ. Chem. Eng. 8 (1), 103647.
Saberian, M., Khabiri, M.M., 2017. Experimental and numerical study of the effects of coal on pavement performance in mine haul road. Geotech. Geol. Eng. 35 (5), 2467–2478.
Saberian, M., Li, J., Nguyen, B.T., Boroujeni, M., 2020. Experimental and analytical study of dynamic properties of UGM materials containing waste rubber. Soil Dynam. Earthq. Eng. 130, 105978.
Saberian, M., Li, J., Perera, S.T.A.M., Zhou, A., Roychand, R., Ren, G., 2021a. Large-scale direct shear testing of waste crushed rock reinforced with waste rubber as pavement base/subbase materials. Transport. Geotech. 28, 100546.
Saberian, M., Li, J., Kilmartin-Lynch, S., Boroujeni, M., 2021b. Repurposing of COVID-19 single-use face masks for pavements base/subbase. Sci. Total Environ. 769, 145527.
Safe Work Australia, 2020. Who should wear gloves to protect against COVID-19? February 16, 2021. https://covid19.swa.gov.au/covid-19-information-workplaces/industry-information/hospitality/gloves.
Sangkham, S., 2020. Face mask and medical waste disposal during the novel COVID-19 pandemic in Asia. Case Stud. Chem. Environ. Eng. 2, 100052.
Sarkodie, S.A., Owusu, P.A., 2021. Impact of COVID-19 pandemic on waste management. Environ. Dev. Sustain. 23 (5), 7951–7960.
Sefouhi, L., Kalla, M., Bahmed, L., Aouragh, L., 2013. The risk assessment for the healthcare waste in the hospital of Batna city, Algeria. Int. J. Environ. Sustain Dev. 4 (4), 442.
Sharma, H.B., Vanapalli, K.R., Cheela, V.S., Ranjan, V.P., Jaglan, A.K., Dubey, B., Goel, S., Bhattacharya, J., 2020. Challenges, opportunities, and innovations for effective solid waste management during and post COVID-19 pandemic. Resour. Conserv. Recycl. 162, 105052.
Shen, T., Xing, S., Wang, S., Cheng, M., Huang, W., 2017. Complex ameliorants screening for reducing swelling ratio and improving shear strength of strong expansive soil. Trans. Chin. Soc. Agric. Eng. 33 (2), 109–115.
Shobana, K.S., Jhanani, S.K., Kumar, B.A., Sarenikashree, V., Saranya, S., 2021. Soil stabilisation using banana fibre and disposable face masks. Int. J. Res. Eng. Sci. Manag. 4 (5), 120–122.
Silva, A.L.P., Prata, J.C., Walker, T.R., Duarte, A.C., Ouyang, W., Barcelò, D., Rocha-Santos, T., 2021. Increased plastic pollution due to COVID-19 pandemic: challenges and recommendations. Chem. Eng. J. 405, 126683.
Singh, V.K., Bommireddy, D.B., Phanikumar, B.R., 2016. Innovative techniques in road and rail construction on expansive soils. SSRG Int. J. Civil Eng. 3 (7), 17–23.
Soundara, B., 2015. Effect of fibres on properties of clay. Int. J. Eng. Appl. Sci. 2 (5), 257909.
Steinberg, M., 2000. Expansive soils and the geomembrane remedy. In: Advances in Unsaturated Geotechnics, pp. 456–466.
Sun, D.A., Zhang, L., Li, J., Zhang, B., 2015. Evaluation and prediction of the swelling pressures of GMZ bentonites saturated with saline solution. Appl. Clay Sci. 105–106, 207–216.
Tang, C., Shi, B., Gao, W., Chen, F., Cai, Y., 2007. Strength and mechanical behavior of short polypropylene fibre reinforced and cement stabilised clayey soil. Geotext. Geomembranes 25 (3), 194–202.
Telugunta, R., Choudhary, S., Sumant, O., 2021. Gloves Market by Type (Disposable Sterile Gloves, Disposable Examination and Protective Gloves, and Consumer Gloves), and Industry (Medical, Horeca (Food), Cleaning, Beauty, Food and Drinks, Pharmaceutical, Chemical, Automotive, Electronics, Construction, and Others): Global Opportunity Analysis and Industry Forecast 2021–2025, 29th July 2022. https://www.alliedmarketresearch.com/gloves-market-A08867.
Tiwari, N., Satyam, N., Patva, J., 2020. Engineering characteristics and performance of polypropylene fibre and silica fume treated expansive soil subgrade. Int. J. Geosynth. Ground Eng. 6 (2), 1–11.
Van Doremalen, N., Bushmaker, T., Morris, D.H., Holbrook, M.G., Gamble, A., Williamson, B.N., Tamin, A., Harcourt, J.L., Thornburg, N.J., Gerber, S.I., Lloyd-Smith, J.O., De Wit, E., Munster, V.J., 2020. Aerosol and surface stability of SARS-CoV-2 as compared with SARS-CoV-1. N. Engl. J. Med. 382 (16), 1564–1567.
Wang, G., Li, J., Saberian, M., Rahat, M.H.H., Massarra, C., Buckhalter, C., Farrington, J., Collins, T., Johnson, J., 2022. Use of COVID-19 Single-Use Face Masks to Improve the Rutting Resistance of Asphalt Pavement. Science of the Total Environment, 154118.
WHO, 2020. Shortage of Personal Protective Equipment Endangering Health Workers Worldwide. Retrieved Retrieved July 07, 2022. https://www.who.int/news/item/03-03-2020-shortage-of-personal-protective-equipment-endangering-health-workers-worldwide.
WHO, 2022. WHO Coronavirus (COVID-19) Dashboard. March 2, 2022. https://covid19.who.int/.
Xiang, Y., Song, Q., Gu, W., 2020. Decontamination of surgical face masks and N95 respirators by dry heat pasteurisation for one hour at 70 C. Am. J. Infect. Control 48 (8), 880–882.
Yadav, J.S., Tiwari, S.K., 2017. Effect of waste rubber fibres on the geotechnical properties of clay stabilized with cement. Appl. Clay Sci. 149, 97–110.
Yarbaşi, N., Kalkan, E., 2020. The mechanical performance of clayey soils reinforced with waste PET fibres. Int. J. Earth Sci. Knowl. Appl. 2 (1), 19–26.
Zaimoglu, A.S., Yetimoglu, T., 2012. Strength behavior of fine grained soil reinforced with randomly distributed polypropylene fibres. Geotech. Geol. Eng. 30 (1), 197–203.
Zheng, J.L., Zhang, R., Yang, H.P., 2009. Highway subgrade construction in expansive soil areas. J. Mater. Civ. Eng. 21 (4), 154–162.
Zumrawi, M.M., 2015. Construction problems of light structures founded on expansive soils in Sudan. Int. J. Sci. Res. 4 (8), 896–902.